

Photoinduced Radical Formation from the Complexes [Re(R)(CO)₃(4,4'-Me₂-bpy)] (R = CH₃, CD₃, Et, ⁱPr, Bz): A Nanosecond Time-Resolved Emission, UV–Vis and IR Absorption, and FT-EPR Study

Cornelis J. Kleverlaan,[†] Derk J. Stufkens,^{*,†} Ian P. Clark,[‡] Michael W. George,[‡]
James J. Turner,[‡] Débora M. Martino,^{§,||} Hans van Willigen,[§] and Antonín Vlček, Jr.^{||}

Contribution from the Anorganisch Chemisch Laboratorium, Institute of Molecular Chemistry, Universiteit van Amsterdam, Nieuwe Achtergracht 166, 1018 WV Amsterdam, The Netherlands, Department of Chemistry, University of Nottingham, University Park, Nottingham, NG7 2RD, U.K., Department of Chemistry, University of Massachusetts at Boston, Boston, Massachusetts 02125, and Department of Chemistry, Queen Mary and Westfield College, University of London, Mile End Road, London, E1 4NS, U.K.

Received February 17, 1998

Abstract: Irradiation of the complexes [Re(R)(CO)₃(dmb)] (R = CH₃, CD₃, Et, ⁱPr, or Bz; dmb = 4,4'-dimethyl-2,2'-bipyridine) into their visible absorption band gives rise to a homolytic cleavage of the Re–R bond with formation of the radicals [Re(CO)₃(dmb)][•] and R[•]. In the case of R = Et, ⁱPr, or Bz this reaction proceeds with unit efficiency. The nanosecond time-resolved absorption (TA) spectra show that the long-lived ($\tau = 7 \mu\text{s}$) [Re(CO)₃(dmb)][•] radicals are formed within the 7 ns laser pulse. The CH₃ complex photodecomposes with a quantum yield of only 0.4. The time-resolved UV–vis and IR absorption spectra reveal that this complex, after excitation into a ¹MLCT state, may either pass a barrier of 1560 cm⁻¹ to the dissociative ³ $\sigma\pi^*$ state and decompose into radicals or decay to the ground state via an excited-state having predominant ³MLCT state character. Qualitative potential energy diagrams are presented for the two types of complexes. In a glass at 80 K and in a low-temperature solution ($T < 195 \text{ K}$), the methyl complex is photostable, and this allowed us to study its excited-state properties with time-resolved absorption, emission, and IR spectroscopies. According to these spectra the lowest-excited ³MLCT state has a significant admixture of a $\sigma\pi^*$ character. Finally, nanosecond time-resolved FT-EPR spectra were recorded of the CH₃ and CD₃ radicals produced by irradiation of [Re(CH₃/CD₃)(CO)₃(dmb)]. The spectra of the CH₃ radical exhibit a pronounced low-field emission/high-field absorption pattern due to an ST₀ radical pair mechanism (RPM) CIDEP effect. The occurrence of this ST₀ RPM confirms that the radicals are formed from an excited state, having spin-triplet character, in agreement with the proposed mechanism involving a reactive ³ $\sigma\pi^*$ state.

Introduction

The organometallic complexes [Re(L')(CO)₃(α -diimine)]^{0/+}, in which L' represents, e.g., Cl⁻ or a N- or P-donor ligand, show strong $d_{\pi}(\text{Re}) \rightarrow \pi^*(\alpha\text{-diimine})$ metal-to-ligand charge transfer (MLCT) transitions in the visible region.^{1–5} Irradiation into these transitions does not give rise to a photochemical reaction, since the transfer of charge from the metal to the α -diimine hardly affects the metal–ligand bonds. Because of their photostability, these complexes are used for photoinduced energy- and electron-transfer processes.^{6,7} Variation of L'

influences the excited-state properties of these Re complexes.⁸ Thus, replacement of Cl⁻ by I⁻ changes the excited-state character from MLCT to XLCT (X = halide),⁹ while the MLCT emission is quenched when L' is an oxidizable donor molecule (D).⁴ In this case, MLCT excitation is followed by an intramolecular electron transfer from D to rhenium whereby the complex arrives in a donor to α -diimine charge transfer state. Direct optical electron transfer from D to the α -diimine does normally not occur due to the lack of overlap between the orbitals involved in this transition.

A special situation arises when the donor ligand in the axial position is covalently bound to rhenium via a high-energy σ -bonding orbital. Following the $d_{\pi} \rightarrow \pi^*(\alpha\text{-diimine})$ (MLCT) excitation, an electron redistribution between the $d_{\pi}(\text{Re})$ and $\sigma(\text{Re}-\text{L}')$ orbitals may take place, whereby the complex arrives in a ³ $\sigma(\text{Re}-\text{L}')\pi^*$ state. From this latter state most complexes undergo a homolytic splitting of the $\sigma(\text{Re}-\text{L}')$ bond with

[†] Universiteit van Amsterdam.

[‡] University of Nottingham.

[§] University of Massachusetts at Boston.

^{||} On leave from the Physics Department, FBCB, UNL, 3000 Santa Fe, Argentina.

(1) Stufkens, D. J. *Comments Inorg. Chem.* **1992**, *13*, 359.

(2) Perkins, T. A.; Humer, W.; Netzel, T. L.; Schanze, K. S. *J. Phys. Chem.* **1990**, *94*, 2229.

(3) Chen, P.; Westmoreland, T. D.; Danielson, E.; Schanze, K. S.; Anthon, D.; Neveux, P. E., Jr.; Meyer, T. J. *Inorg. Chem.* **1987**, *26*, 1116.

(4) Schanze, K. S.; MacQueen, D. B.; Perkins, T. A.; Cabana, L. A. *Coord. Chem. Rev.* **1993**, *122*, 63.

(5) Worl, L. A.; Duesing, R.; Chen, P.; Ciana, L. D.; Meyer, T. J. *J. Chem. Soc., Dalton Trans.* **1991**, 849.

(6) Wrighton, M. S.; Morse, D. L. *J. Am. Chem. Soc.* **1974**, *96*, 998.

(7) Luong, J. C.; Nadjo, L.; Wrighton, M. S. *J. Am. Chem. Soc.* **1978**, *100*, 5790.

(8) Stufkens, D. J.; Vlček, A., Jr. *Coord. Chem. Rev.* in press.

(9) Rossenaar, B. D.; Stufkens, D. J.; Vlček, A., Jr. *Inorg. Chem.* **1996**, *35*, 2902.

formation of radicals. In recent years we have studied several complexes of the type $[\text{Re}(\text{L}')(\text{CO})_3(\alpha\text{-diimine})]$ in which L' represents a metal fragment ($\text{L}' = \text{Mn}(\text{CO})_5$, $\text{Re}(\text{CO})_5$, $\text{Co}(\text{CO})_4$, $\text{FeCp}(\text{CO})_2$, or SnPh_3)^{1,10–24} or an alkyl or benzyl (Bz) ligand.^{25–29} These studies have shown that all metal–metal bonded complexes possess such a high-energy $\sigma(\text{M}–\text{Re})$ orbital and, as a result, a lowest $^3\sigma\pi^*$ excited state. With the exception of the $[\text{Re}(\text{SnPh}_3)(\text{CO})_3(\alpha\text{-diimine})]$ complexes,²³ which have a very strong Re–Sn bond, all of these compounds undergo a homolysis of the metal–metal bond from their $^3\sigma\pi^*$ state.

The situation is different for the corresponding alkyl or benzyl complexes $[\text{Re}(\text{R})(\text{CO})_3(\alpha\text{-diimine})]$ ($\text{R} = \text{CH}_3$, CD_3 , Et, ⁱPr, Bz). According to its UV photoelectron spectrum,²⁵ the complex $[\text{Re}(\text{CH}_3)(\text{CO})_3(\text{Pr-DAB})]$ (Pr-DAB = *N,N'*-diisopropyl-1,4-diazabutadiene) has its $\sigma(\text{Re}–\text{CH}_3)$ orbital at a lower energy than the $d_\pi(\text{Re})$ orbitals in which the MLCT transitions originate. As a result the reactive $^3\sigma\pi^*$ state will be at higher energy than the MLCT states and the complex is not expected to be very photoreactive. Photochemical studies of the $[\text{Re}(\text{R})(\text{CO})_3(\text{Pr-DAB})]$ ($\text{R} = \text{CH}_3$, Et, or Bz) complexes indeed revealed that, contrary to the ethyl and benzyl complexes, the methyl compound is hardly photoreactive.²⁵ The quantum yield (Φ) for the homolysis of the Re–CH₃ bond is only $(1–3) \times 10^{-2}$, whereas it is close to unity for the corresponding Et and Bz complexes.²⁵ It is noteworthy that for the methyl complex Φ increases with the energy of excitation within the MLCT band, while at the same time the activation energy E_a decreases. This implies^{30–32} that the reactive $^3\sigma\pi^*$ state is populated from the optically excited Franck–Condon levels of the ¹MLCT state, in competition with their fast relaxation.

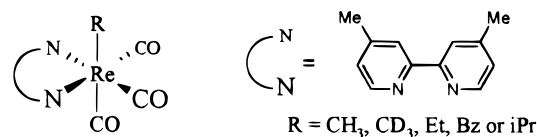


Figure 1. General molecular structure of *fac*- $[\text{Re}(\text{R})(\text{CO})_3(\text{dmb})]$ and the α -diimine ligand dmb.

To understand the chemical reactivity and dynamics of the $\sigma\pi^*$ excited state and the mechanism of its population after the optical MLCT excitation, we have started a photochemical and photophysical study of the complexes $[\text{Re}(\text{R})(\text{CO})_3(\text{dmb})]$ ($\text{R} = \text{CH}_3$, CD_3 , Et, ⁱPr, and Bz; dmb = 4,4'-dimethyl-2,2'-bipyridine). They are expected to have rather long lifetimes in their ³MLCT states because of the rigidity and high π^* orbital energy of the dmb ligand. As will be demonstrated in this paper, the $[\text{Re}(\text{R})(\text{CO})_3(\text{dmb})]$ ($\text{R} = \text{CH}_3$, CD_3) complex allows us to study in detail the competition between the unproductive decay to the ground state and the radical formation. This information is mainly derived from the nanosecond time-resolved emission, and UV–vis and infrared absorption spectra, measured at various temperatures and in different media. To establish the spin character of the reactive state from which the methyl radicals are produced and to determine for the first time the spin–lattice relaxation of these radicals at room temperature, we have also performed a nanosecond time-resolved FT-EPR study of the complexes $[\text{Re}(\text{R})(\text{CO})_3(\text{dmb})]$ ($\text{R} = \text{CH}_3$, CD_3). The schematic structures of the complexes and of the dmb ligand are presented in Figure 1.

Experimental Section

Materials and Preparations. The complexes $[\text{Re}(\text{R})(\text{CO})_3(\text{dmb})]$ ($\text{R} = \text{CH}_3$, CD_3 , Et, ⁱPr, and Bz) were prepared according to procedures described elsewhere.³³ They were characterized by FT-IR, UV–vis, and ¹H and ¹³C NMR spectroscopies. Solvents for spectroscopic studies and photochemical experiments were of analytical grade, dried over sodium (THF, 2-MeTHF, toluene) or CaH₂ (CH₂Cl₂) and distilled under a N₂ atmosphere. The solvents EtCN, PrCN, and 2-propanol, used for the time-resolved IR and FT-EPR experiments, were degassed and used under an Ar atmosphere. Sample preparations for the various experiments were carried out under an Ar or N₂ atmosphere using Schlenk techniques. The solutions were carefully handled in the dark before the experiments were performed.

Spectroscopic and Photochemical Measurements. Electronic absorption spectra were recorded on a Varian Cary 4E spectrophotometer; infrared spectra were obtained on a Bio-Rad FTS-60A FTIR spectrometer equipped with a liquid nitrogen-cooled MCT detector.

Quantum yields of the photoreactions were obtained by studying the disappearance of the parent complexes via the decay of their visible absorption band. For this purpose the sample was irradiated within the spectrophotometer with one of the laser lines of an SP2025 argon-ion laser via an optical fiber and a computer-controlled mechanical shutter. Light intensities were measured with a Coherent model 212 power meter, which was calibrated with an Aberchrome 540 and 540 P solution according to literature methods.^{34,35} The 1 cm sample cuvette was kept at a constant temperature, and the solution was vigorously stirred during the measurements. The sample concentration was adjusted to keep the maximum absorbance of the visible absorption band between 1.0 and 1.2. The irradiation time intervals were chosen in such a way that the conversion in each irradiation step was less than 5%. The quantum yields reported are average values of several measurements. Typical incident light intensities at the irradiation wavelength were $(8–13) \times 10^{-9}$ einstein s⁻¹. The program used to

(10) Luong, J. C.; Faltynek, R. A.; Wrighton, M. S. *J. Am. Chem. Soc.* **1980**, *102*, 7892.

(11) Luong, J. C.; Faltynek, R. A.; Wrighton, M. S. *J. Am. Chem. Soc.* **1979**, *101*, 1597.

(12) Morse, D. L.; Wrighton, M. S. *J. Am. Chem. Soc.* **1976**, *98*, 3931.

(13) Kokkes, M. W.; Stufkens, D. J.; Oskam, A. *Inorg. Chem.* **1985**, *24*, 2934.

(14) Kokkes, M. W.; De Lange, W. G. J.; Stufkens, D. J.; Oskam, A. *J. Organomet. Chem.* **1985**, *294*, 59.

(15) Kokkes, M. W.; Stufkens, D. J.; Oskam, A. *Inorg. Chem.* **1985**, *24*, 4411.

(16) Stufkens, D. J. *Coord. Chem. Rev.* **1990**, *104*, 39.

(17) Andréa, R. R.; de Lange, W. G. J.; Stufkens, D. J.; Oskam, A. *Inorg. Chem.* **1989**, *28*, 318.

(18) van Dijk, H. K.; van der Haar, J.; Stufkens, D. J.; Oskam, A. *Inorg. Chem.* **1989**, *28*, 75.

(19) van der Graaf, T.; Stufkens, D. J.; Oskam, A.; Goubitz, K. *Inorg. Chem.* **1991**, *30*, 599.

(20) van der Graaf, T.; van Rooy, A.; Stufkens, D. J.; Oskam, A. *Inorg. Chim. Acta* **1991**, *187*, 133.

(21) van Outersterp, J. W. M.; Stufkens, D. J.; Vlček, A., Jr. *Inorg. Chem.* **1995**, *34*, 5183.

(22) Rossenaar, B. D.; van der Graaf, T.; van Eldik, R.; Langford, C. H.; Stufkens, D. J.; Vlček, A., Jr. *Inorg. Chem.* **1994**, *33*, 2865.

(23) Rossenaar, B. D.; Lindsay, E.; Stufkens, D. J.; Vlček, A., Jr. *Inorg. Chim. Acta* **1996**, *250*, 5.

(24) Servaas, P. C.; Stor, G. J.; Stufkens, D. J.; Oskam, A. *Inorg. Chim. Acta* **1990**, *178*, 185.

(25) Rossenaar, B. D.; Kleverlaan, C. J.; van de Ven, M. C. E.; Stufkens, D. J.; Vlček, A., Jr. *Chem. Eur. J.* **1996**, *2*, 228.

(26) Rossenaar, B. D.; Kleverlaan, C. J.; van de Ven, M. C. E.; Stufkens, D. J.; Oskam, A.; Fraanje, J.; Goubitz, K. *J. Organomet. Chem.* **1995**, *493*, 153.

(27) Rossenaar, B. D.; George, M. W.; Johnson, F. P. A.; Stufkens, D. J.; Turner, J. J.; Vlček, A., Jr. *J. Am. Chem. Soc.* **1995**, *117*, 11582.

(28) Kleverlaan, C. J.; Martino, D. M.; van Willigen, H. v.; Stufkens, D. J.; Oskam, A. *J. Phys. Chem.* **1996**, *100*, 18607.

(29) Lucia, L. A.; Burton, R. D.; Schanze, K. S. *Inorg. Chim. Acta* **1993**, *208*, 103.

(30) Vlček, A., Jr. *Coord. Chem. Rev.*, in press.

(31) Vlček, A., Jr.; Vichová, J.; Hartl, F. *Coord. Chem. Rev.* **1994**, *132*, 167.

(32) Vichová, J.; Hartl, F.; Vlček, A., Jr. *J. Am. Chem. Soc.* **1992**, *114*, 10903.

(33) Kleverlaan, C. J.; Stufkens, D. J. *Inorg. Chim. Acta* In press.

(34) Kuhn, H. J.; Braslavsky, S. E.; Schmidt, R. *Pure Appl. Chem.* **1989**, *61*, 187.

(35) Heller, H. G.; Langan, J. R. *J. Chem. Soc., Perkin Trans. 2* **1981**, 341.

calculate the quantum yield corrects for the changes in the light absorption by the parent compound caused both by its depletion and by the inner filter effect of the photoproduct, according to a procedure reported previously.^{32,36}

Nanosecond time-resolved electronic absorption spectra were obtained by irradiating the sample with 7 ns pulses (fwhm) of a Spectra Physics GCR-3 Nd:YAG laser working at 10 Hz. The desired excitation wavelength was selected by frequency tripling of the 1064 nm fundamental (355 nm), or by using a Quanta-Ray PDL-pulsed dye laser (Spectra Physics) with a suitable dye (Coumarine 440) pumped by the third harmonic frequency of the Nd:YAG laser. Typical energies were 10 mJ/pulse for all excitation wavelengths. The concentration of the solution was such that the absorbance at the excitation wavelength was between 0.5 and 1.0 and the maximum absorbance did not exceed 1.5. An EG&G FX-504 high power lamp with a PS-302 power supply was used as the probe source. After the sample was passed, the probe light was transferred via an optical fiber to a spectrograph (Acton Spectrapro 150s imaging spectrograph) equipped with a 150 g/mm or 600 g/mm grating and a variable slit (1–500 μm) resulting in 6 nm (150 g/mm) or 1.2 nm (600 g/mm) as the maximum resolution. The data collection system further consisted of a Princeton Instruments model ICCD-576EMG/RB detector and a Princeton Instruments Programmable Pulse Generator model PG-200. An EG&G Princeton Applied Research Digital Delay Generator model 9650 was used as the pulse programmer, controlling the probe light, the laser, and the pulse generator for the CCD detector. The pump and probe beams were focused perpendicularly on the sample. In the case of the photostable compounds, a 1 cm fluorescence cuvette was used, for the photolabile complexes a homemade flowcell and a Verder 2040 pump. The flow speed was ca. 40 mL/min affording a fresh sample every 10 ms after excitation. A home-built cuvette was used for the low-temperature transient absorption spectra. The same setup (without the flash lamp) was employed for the low-temperature time-resolved emission experiments. The complex was dissolved in freshly distilled 2-MeTHF (ca. 10^{-4} M), and this solution was freeze–pump–thaw degassed in a cylindrical glass tube (diameter 1 cm) at least three times, which was then sealed under vacuum. Both the low-temperature transient absorption and emission spectroscopic measurements were performed in an Oxford Instruments DN 1704/54 liquid nitrogen cryostat. The emission lifetimes were calculated by fitting the emission intensity measured at at least 10 different delay times after the laser excitation. This was repeated for at least 10 different wavelengths, and the calculated lifetimes were averaged. Emission quantum yields were measured relative to a standard solution of [Re(Cl)(CO)₃(bpy)] in 2-MeTHF ($\Phi_s = 0.028$ at 77 K),⁵ using a 1 ms gate.

The time-resolved IR (TRIR) spectra were studied at the University of Nottingham, U.K. The details of the setup are described elsewhere.^{37,38} The third harmonic frequency (355 nm, 7 ns fwhm) of a Quanta-Ray GCR-12S Nd:YAG laser was used to excite the sample. An infrared diode laser (Mütek MSD 1100) was used as the IR probe. It was tuned between 1840 and 2050 cm^{-1} . The changes in the IR absorption at a selected wavenumber were monitored with a photo-voltaic 77 K MCT detector (Laser Monitoring Systems PV 2180) having a rise time of approximately 50 ns. Kinetic traces obtained at different wavenumbers were used to construct the transient IR spectra point by point at given time delays. The sample solution was refreshed after each four laser flashes. Low-temperature TRIR measurements (77 K) were performed in a home-built cryostat.

Time-resolved FT-EPR measurements were carried out using a home-built spectrometer.^{39,40} The response of the sample to the $\pi/2$ microwave pulses was detected in quadrature with application of the CYCLOPS phase cycling routine. Solutions of the complexes (ca. 2 mM) were freed of oxygen by purging with nitrogen prior to and during

Table 1. Quantum Yields and Activation Energies (E_a)^a of the Photochemical Homolysis of [Re(R)(CO)₃(dmb)] (R = CH₃, Bz) in Toluene as a Function of the Irradiation Wavelength and Temperature

T (K)	R = CH ₃		R = Bz	
	457.9 nm	488.0 nm	488.0 nm	514.5 nm
303	0.61	0.61		
293		0.42	1.07	0.86
283		0.36		
273		0.31	0.96	0.73
263		0.16		
253		0.13	0.90	0.66
E_a (cm^{-1})		1560	215	330

^a Estimated error ca. 15%.

the measurements. The solutions were pumped through a quartz EPR flow cell held in the microwave cavity and excited with the third harmonic (355 nm) of a Quanta Ray GCR12 Nd:YAG laser (pulse width 8 ns, pulse energy ~ 20 mJ, pulse repetition rate 10 Hz). All measurements were performed at room temperature. The time evolution of the transient spectra was measured as follows. The FID produced by a $\pi/2$ (15 ns) microwave pulse was recorded for a series of delay times τ_d (10 ns to 1.5 μs) between laser and microwave pulses. Amplitudes, line widths, and phases of resonance peaks were then calculated from the FIDs with a LPSVD analysis routine.⁴¹ Since the spectra cover a frequency range that far exceeds the band width of the spectrometer, EPR spectra presented in the figures are assembled from FIDs obtained with a set of distinct field values. Corrections for the variation in signal intensity with change in frequency offset were based on calibration data given by a stable free radical reference.

Results

The complexes [Re(R)(CO)₃(dmb)] all possess a rather strong absorption band ($\epsilon = (2.5\text{--}3.0) \times 10^3 \text{ M}^{-1} \text{ cm}^{-1}$) between 400 and 500 nm. According to its solvatochromic behavior, and the resonance Raman data obtained for the representative complexes [Re(R)(CO)₃(dmb)] (R = CH₃ or CD₃),³³ this band was assigned to one or more MLCT transitions. It would have been preferable to study the photochemistry and photophysics of these complexes by irradiation into this absorption band. This was, however, not possible in the case of the time-resolved IR and FT-EPR spectra since the complexes did not absorb the 532 nm line of the Nd:YAG laser and the appropriate dye laser for excitation in the 400–500 nm region was not available. Therefore, the 355 nm line was used for excitation in the IR and FT-EPR measurements. It will become evident that excitation with 355 nm still populates the lowest excited state of the complexes under study, even in a glass at 77K.

Quantum Yields. Irradiation of a complex [Re(R)(CO)₃(dmb)] (R = alkyl or benzyl) in CH₂Cl₂, CHCl₃, or CCl₄/CH₂-Cl₂ (1:10 v/v) affords [Re(Cl)(CO)₃(dmb)] as the only Re-containing photoproduct independent of R.^{29,33} In toluene different products were obtained, viz. the solvated radical species [Re(Sv)(CO)₃(dmb)]* (Sv = Solvent) and the cationic complex [Re(Sv)(CO)₃(dmb)]⁺.³³ In this study the efficiencies of these photoreactions were determined by measuring the quantum yield (Φ) of the disappearance of the parent complex in toluene as a function of excitation wavelength and temperature. The quantum yields obtained for [Re(R)(CO)₃(dmb)] (R = CH₃ and Bz) are summarized in Table 1. The quantum yield of the photolysis of [Re(CH₃)(CO)₃(dmb)] shows a pronounced Arrhenius-type exponential dependence on the temperature with an activation

(41) de Beer, R.; van Ormondt, D. *Advanced EPR: Applications in Biology and Biochemistry*; Hoff, A. J., Ed.; Elsevier: Amsterdam, The Netherlands, 1989.

(36) Manuta, D. M.; Lees, A. J. *Inorg. Chem.* **1986**, *25*, 1354.

(37) Nieuwenhuis, H. A.; Stufkens, D. J.; McNicholl, R.-A.; Al-Obaidi, A. H. R.; Coates, C. G.; Bell, S. E. J.; McGarvey, J. J.; Westwell, J.; George, M. W.; Turner, J. J. *J. Am. Chem. Soc.* **1995**, *117*, 5579.

(38) George, M. W.; Poliakoff, M.; Turner, J. J. *Analyst* **1994**, *551*.

(39) Levstein, P. R.; van Willigen, H. *J. Chem. Phys.* **1991**, *95*, 900.

(40) van Willigen, H.; Levstein, P. R.; Ebersole, M. H. *Chem. Rev.* **1993**, *93*, 173.

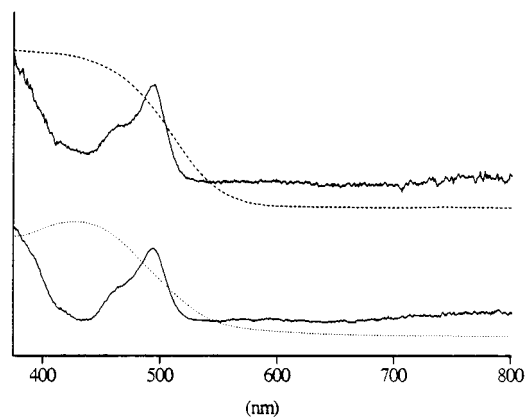


Figure 2. Time-resolved difference UV-vis absorption spectra of the $[\text{Re}(\text{THF})(\text{CO})_3(\text{dmb})]^*$ radicals measured 10 ns after the laser pulse excitation of $[\text{Re}(\text{Bz})(\text{CO})_3(\text{dmb})]$ (top) and $[\text{Re}(\text{Et})(\text{CO})_3(\text{dmb})]$ (bottom) in THF at 293 K. The dashed lines represent the ground-state absorption spectra of the starting complexes; the full lines the differences between the spectra measured after and before the excitation. Laser pulses of 355 nm (7 ns) were used for excitation.

energy of ca. 1560 cm^{-1} . A much lower activation energy, ca. 215 cm^{-1} , was determined for the $[\text{Re}(\text{Bz})(\text{CO})_3(\text{dmb})]$ complex.

Time-Resolved UV-Vis Absorption and Emission Spectra. To determine the character and dynamics of the photochemically relevant excited states, a flash photolysis study with UV-vis detection was carried out in the nanosecond to microsecond time range. In these experiments, a solution of the $[\text{Re}(\text{R})(\text{CO})_3(\text{dmb})]$ complex was excited at 440 or 355 nm. The transient absorption (TA) spectra were recorded at different delay times after the laser pulse, with a gating of 5–10 ns. Variation of the excitation wavelength had no influence on the shape and lifetimes of the transient absorption.

The type of TA spectra observed for these complexes depends on the alkyl ligand R. In general, the behavior of the complexes containing $\text{R} = \text{Et}$, Bz , or $i\text{Pr}$ differ from that of $[\text{Re}(\text{CH}_3)(\text{CO})_3(\text{dmb})]$. The difference absorption spectra obtained 5 ns after the 355 or 440 nm excitation of a THF solution of the complexes $[\text{Re}(\text{R})(\text{CO})_3(\text{dmb})]$ ($\text{R} = \text{Et}$, Bz , or $i\text{Pr}$) show a strong transient absorption with an apparent maximum at ca. 500 nm (see Figure 2). The position and shape of this absorption depend neither on R ($\text{R} = \text{Et}$, Bz , or $i\text{Pr}$) nor on the solvent (toluene, CH_2Cl_2 or THF), and the absorption stays constant during the next 100 ns. On a longer time scale (μs), this transient disappears while the bleaching of the absorption due to the parent complex remains. The lifetime of the transient is approximately $7\ \mu\text{s}$ in THF or toluene and $5\ \mu\text{s}$ in CH_2Cl_2 . It is independent of the alkyl ligand used. On the basis of its long lifetime, the independence of its properties on R, the close correspondence between its UV-vis and IR (vide infra) absorption spectra with those of the reduction product of $[\text{Re}(\text{Br})(\text{CO})_3(\text{dmb})]$,⁴² this transient species is identified as the $[\text{Re}(\text{Sv})(\text{CO})_3(\text{dmb})]^*$ radical.

The time-resolved UV-vis spectra of the complexes $[\text{Re}(\text{R})(\text{CO})_3(\text{dmb})]$ ($\text{R} = \text{CH}_3$ or CD_3) excited at 355 or 440 nm differ from those obtained for the complexes with $\text{R} = \text{Et}$, Bz , or $i\text{Pr}$, as shown by a comparison of Figures 2 and 3. Directly after laser excitation, both methyl compounds show transient spectra with two apparent maxima at 520 and 485 nm, respectively, and a strong absorption below 400 nm. The absorption at about 520 nm and in the UV region decays with

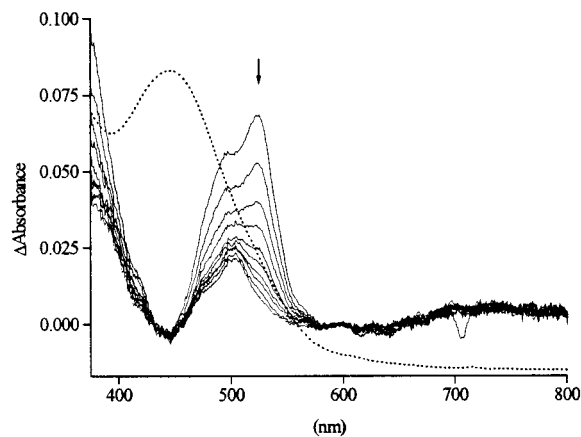


Figure 3. Time-resolved difference UV-vis absorption spectra obtained by excitation of $[\text{Re}(\text{CH}_3)(\text{CO})_3(\text{dmb})]$ in toluene at 293 K with 355 nm (7 ns) laser pulses. The dashed line is the ground-state absorption spectrum; the full lines represent the differences between the spectra measured at different delay times ($\tau_d = 10, 20, 30, 40, 50, 60, 70, 80, 90,$ and 100 ns , respectively) after the pulse and before the excitation.

Table 2. Lifetimes of the Excited State of $[\text{Re}(\text{CH}_3)(\text{CO})_3(\text{dmb})]$ in Various Solvents Measured by Time-Resolved Absorption Spectroscopy ($\lambda_{\text{exc}} = 355\text{ nm}$)

solvent	lifetime (ns)
10% (v/v) $\text{CCl}_4/\text{CH}_2\text{Cl}_2$ (rt)	20
CH_2Cl_2 (rt)	35
toluene (rt)	40
THF (rt)	30
2-MeTHF (123 K)	1.0×10^3

a slightly solvent-dependent lifetime (40–20 ns, see Table 2) leaving a residual absorption spectrum that shows a maximum at about 500 nm, identical with that of the photoproduct of the Et, $i\text{Pr}$, or Bz complexes. The latter absorption decays with a lifetime of $7\ \mu\text{s}$, while bleaching of the ground state remains. Obviously, the initial TA spectrum consists of two overlapping absorptions, one of which is due to the long-lived $[\text{Re}(\text{Sv})(\text{CO})_3(\text{dmb})]^*$ radical. The other absorption decays with a lifetime of ca. 40 ns. It is assigned to a $^3\text{MLCT}$ excited state, since it closely resembles the transient absorption of the photostable complex $[\text{Re}(\text{Cl})(\text{CO})_3(\text{bpy})]$.⁵ Both the radical photoproduct and the excited complex molecules are fully formed within the time span of the excitation pulse, 7 ns.

Time-resolved absorption spectra of $[\text{Re}(\text{CH}_3)(\text{CO})_3(\text{dmb})]$ were also recorded in a 2-MeTHF glass at 123 K, under which condition this complex is completely photostable. These spectra (Figure 4) show the presence of a transient species that is characterized by apparent maxima at 510 and 475 nm, resembling the spectrum of $\text{dmb}^{\cdot-}$ anion coordinated in $[\text{Re}(\text{Br})(\text{CO})_3(\text{dmb})]^-$.⁴³ This transient is formed already in the excitation pulse; it decays completely and directly to the ground state with a lifetime of $1\ \mu\text{s}$ (at 123 K) and without formation of any $[\text{Re}(\text{Sv})(\text{CO})_3(\text{dmb})]^*$ radicals. This behavior suggests that this transient absorption belongs to a CT excited state. The shape of the spectra in a 2-MeTHF glass seems to deviate appreciably from that of the spectra measured at room temperature. However, very similar spectra are obtained if we correct both spectra for the bleaching of the ground-state absorption and, in addition, the room temperature spectra for the absorption by the radical. It is noteworthy that the low-energy peak of

(42) Rossenaar, B. D.; Hartl, F.; Stufkens, D. J. *Inorg. Chem.* **1996**, *35*, 6194.

(43) Rossenaar, B. D.; Stufkens, D. J.; Vlček A., Jr. *Inorg. Chim. Acta* **1996**, *247*, 247.

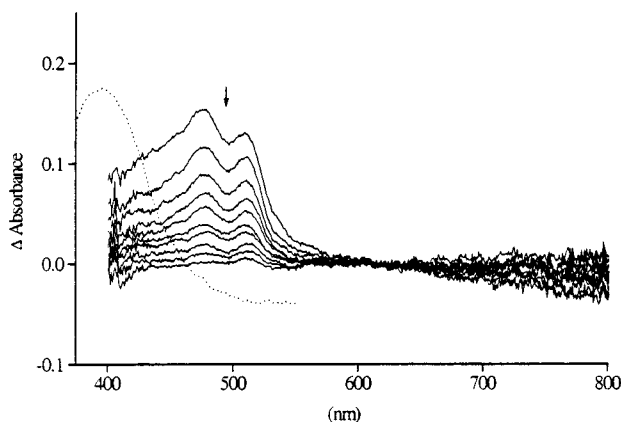


Figure 4. Time-resolved difference UV-vis absorption spectra obtained by excitation of $[\text{Re}(\text{CH}_3)(\text{CO})_3(\text{dmb})]$ in a 2-MeTHF glass at 113 K with 355 nm (7 ns) laser pulses. The dashed line represents the ground-state absorption spectrum; the full lines the differences between the spectrum of the decaying $^3\text{MLCT}$ state of the complex and that of its ground state measured at delay times ranging from 500 ns to 5 μs after the excitation.

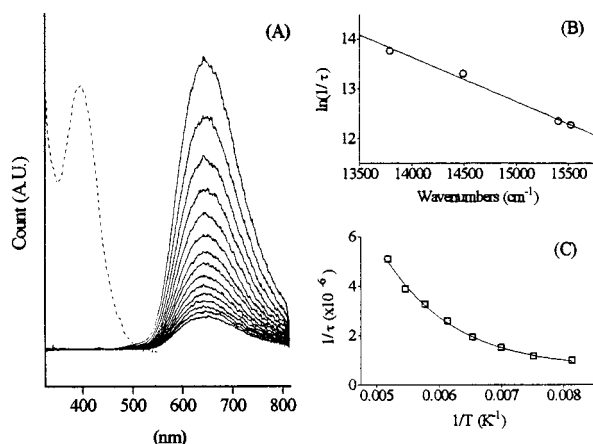


Figure 5. Emission properties of $[\text{Re}(\text{CH}_3)(\text{CO})_3(\text{dmb})]$. (A) Time-resolved emission spectra measured for the complex in a 2-MeTHF glass at 80 K using 440 nm, 7 ns laser pulse excitation. The first spectrum (top) is measured at 500 ns after the excitation, the interval between the following spectra is 1 μs . (B) Correlation between the logarithm of the nonradiative decay rate, approximated by $\ln 1/\tau$, and the emission energy in the temperature region of the glass-to-fluid transition of 2-MeTHF (data from Table 4). Experimental points shown correspond to $T = 113, 103, 93,$ and 83 K. (C) Temperature dependence of the emission lifetime measured for the complex in a fluid 2-MeTHF solution in the 123–193 K range.

the transient absorption only shows a minor shift on cooling. This agrees with the assignment of this band to an intraligand transition of the dmb radical anion, the position of which will hardly depend on the surrounding medium.

Emission spectra were obtained for $[\text{Re}(\text{R})(\text{CO})_3(\text{dmb})]$ ($\text{R} = \text{CH}_3$ or CD_3). Both complexes show the same spectra in a 2-MeTHF glass at low temperatures with a single, unstructured, band with a maximum at 644 nm (Figure 5). The shape and position of the emission, as well as its lifetime, do not depend on the wavelength of excitation ($\lambda_{\text{exc}} = 355$ or 440 nm). The emission data are collected in Table 3, together with those of $[\text{Re}(\text{Ph})(\text{CO})_3(\text{dmb})]$ and $[\text{Re}(\text{Cl})(\text{CO})_3(\text{bpy})]$. The main error is in the emission quantum yield and is estimated to be ca. 15%, taking into account the uncertainty in the reference value (see Experimental Section). The emission lifetime of the methyl complex is temperature dependent (Table 4, Figure 5). An

increase of temperature from 83 to 113 K leads to a decrease of the emission energy caused by the gradual softening of the 2-MeTHF glass, i.e., the glass-to-fluid transition. It is accompanied by a decrease of the emission lifetime, according to the energy gap law.⁴⁴ This is demonstrated in Figure 5B. The emission energy is temperature independent in fluid 2-MeTHF solution above 113 K but the lifetime decreases exponentially with increasing temperature. Experimental data measured over the temperature range of 113–193 K were fitted to eq 1 with the following parameter values: $k_0 = 6.5 \times 10^5 \text{ s}^{-1}$, $A = 4.7 \times 10^8$, and $E_a = 620 \pm 120 \text{ K}$. (Note that k_0 approximately equals the rate of nonradiative decay to the ground state via the weak coupling mechanism, since $k_0 \gg k_r$.) Measurements

$$\frac{1}{\tau} = k_0 + Ae^{(-E_a/RT)} \quad (1)$$

above 193 K were precluded for this complex by sample photodecomposition. The emission spectra of the corresponding complexes $[\text{Re}(\text{R})(\text{CO})_3(\text{dmb})]$ ($\text{R} = \text{Et}, \text{Bz},$ or ^iPr) could not be measured at all due to their photolability, even in a glass at 77 K.

Time-Resolved Infrared Spectra. The UV-vis transient absorption and emission spectra give indirect information on the character of the lowest-excited state and the nature of the primary photoproduct. They do not, however, provide the important structural information that is normally derived from vibrational spectra. Hence, nanosecond time-resolved infrared absorption (TRIR) spectra in the region of the CO-stretching vibrations were studied. $[\text{Re}(\text{CH}_3)(\text{CO})_3(\text{dmb})]$ was selected for these experiments since it is the only complex that shows the simultaneous formation of an excited state and a primary photoproduct. TRIR spectra were measured in a EtCN/PrCN (4:5 v/v) mixture either as a fluid solution in the temperature range of 195–238 K or as a glass at 80 K. The transient IR data are collected in Table 5.

Figure 6 shows the TRIR spectrum of $[\text{Re}(\text{CH}_3)(\text{CO})_3(\text{dmb})]$ measured at 80 K. The spectrum was recorded 500 ns after the 355 nm excitation. It shows a depletion of the three ground-state $\nu(\text{CO})$ bands at 1987, 1874, and 1867 cm^{-1} and the appearance of three new bands at higher frequencies (2014, 1933, and 1903 cm^{-1}). It follows that the excited complex has retained its *fac*-triscarbonyl structure. The increase of the $\nu(\text{CO})$ vibrational frequencies indicates that the excited state has mainly MLCT character since MLCT excitation implies an oxidation of the metal. As a result of this the metal-to-CO π back-bonding is decreased and the CO bonds are strengthened. A similar influence of MLCT excitation on the $\nu(\text{CO})$ wavenumbers has been observed for other metal carbonyls, including $[\text{Re}(\text{Cl})(\text{CO})_3(\text{bpy})]$.^{45–48} The intensities of the IR peaks of both the excited complex and the depleted ground-state decay with the same lifetime of 5 μs , which, in turn is identical to the emission lifetime measured at the same temperature. There is a complete ground-state recovery.

The frequencies of the CO-stretching vibrations of $[\text{Re}(\text{CH}_3)(\text{CO})_3(\text{dmb})]$ in its excited state are sensitive to the rigidity of the medium. Going from the EtCN/PrCN (4:5 v/v) glass at 80 K to the solution at 195 K in this solvent mixture, these frequencies increase from 2014, 1933, and 1903 cm^{-1} to 2029,

(44) Caspar, J. V.; Kober, E. M.; Sullivan, B. P.; Meyer, T. J. *J. Am. Chem. Soc.* **1982**, *104*, 630.

(45) Turner, J. J.; George, M. W.; Johnson, F. P. A.; Westwell, J. R. *Coord. Chem. Rev.* **1993**, *125*, 101.

(46) Schoonover, J. R.; Bignozzi, C. A.; Meyer, T. J. *Coord. Chem. Rev.* **1997**, *165*, 239.

(47) Schoonover, J. R.; Strouse, G. F.; Omberg, K. M.; Dyer, R. B. *Comments Inorg. Chem.* **1996**, *18*, 165.

Table 3. Emission Properties^a (Lifetime τ , Quantum Yield Φ_r , Radiative Rate Constant k_r , and Nonradiative Rate Constant k_{nr}) of the [Re(L)(CO)₃(dmb)] (L = CH₃, Ph) and [Re(Cl)(CO)₃(bpy)] Complexes in a 2-MeTHF Glass at 80 K

compound	λ_{abs} (nm)	λ_{em} (nm)	Stokes shift ΔE (cm ⁻¹) ^b	τ (μ s)	Φ_r ($\times 10^{-4}$)	k_r (s ⁻¹)	k_{nr} ($\times 10^4$ s ⁻¹)
[Re(CH ₃)(CO) ₃ (dmb)] ^c	398 nm	644 nm	9690	5.0	23.3	466	20.0
[Re(Ph)(CO) ₃ (dmb)] ^c	408 nm	608 nm	8060	11.8	131	1110	8.4
[Re(Cl)(CO) ₃ (bpy)] ^d	375 nm	532 nm	7870	2.7	280	10370	36.0

^a Estimated error in Φ_r ca. 15%. ^b Apparent Stokes shift defined as $\Delta E = E_{abs} - E_{em}$. ^c This work. ^d From ref 9.

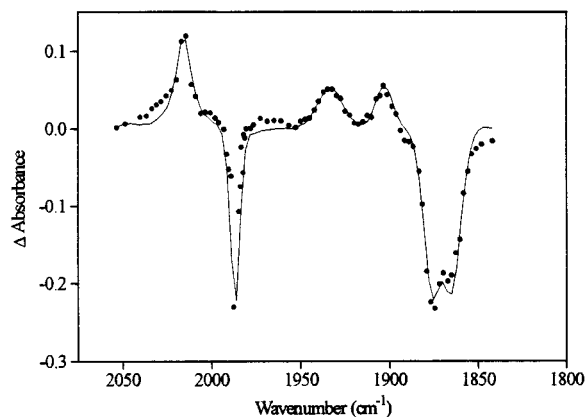
Table 4. Emission Properties of the [Re(CH₃)(CO)₃(dmb)] Complex in a 2-MeTHF Glass and Fluid Solution at Different Temperatures

T (K)	τ (μ s)	λ_{max} (nm)	T (K)	τ (μ s)	λ_{max} (nm)
83	4.73	644	143	0.67	725
93	4.36	647	153	0.52	725
103	1.68	690	163	0.39	725
113	1.06	725	173	0.31	725
123	1.01	725	183	0.26	725
133	0.98	725	193	0.20	725

Table 5. Transient IR Data (CO-Stretching Region) of [Re(CH₃)(CO)₃(dmb)] and Related Complexes in EtCN/PrCN (4:5 v/v)

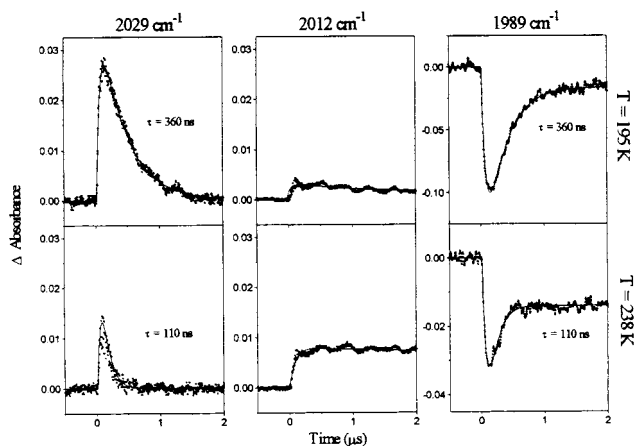
compound	state	T (K)	ν (CO) cm ⁻¹
[Re(CH ₃)(CO) ₃ (dmb)]	G.S.	80	1987, 1874, 1867
[Re(CH ₃)(CO) ₃ (dmb)]	E.S.	80	2014, 1933, 1903
[Re(CH ₃)(CO) ₃ (dmb)]	G.S.	195	1987, 1874, 1867
[Re(CH ₃)(CO) ₃ (dmb)]	E.S.	195	2029, 1950, 1925
[Re(Sv)(CO) ₃ (dmb)] ^a		195	2011, 1899
[Re(Cl)(CO) ₃ (dmb)] ^b	G.S.	77	2020, 1913, 1894
[Re(Cl)(CO) ₃ (dmb)] ^b	E.S.	77	2040, 1971, 1932
[Re(Cl)(CO) ₃ (dmb)] ^b	G.S.	135	2020, 1914, 1895
[Re(Cl)(CO) ₃ (dmb)] ^b	E.S.	135	2066, 1993, 1950

^a From ref 49. ^b From ref 48.

**Figure 6.** Time-resolved difference infrared absorption spectrum (CO-stretching region) of [Re(CH₃)(CO)₃(dmb)] measured 500 ns after the excitation in EtCN/PrCN (4:5 v/v) at 80 K. The spectrum shows the disappearance of the parent complex (negative peaks) and the formation of a transient species (positive bands).

1950, and ca. 1925 cm⁻¹. A similar IR rigidochromic shift has been observed for [Re(Cl)(CO)₃(bpy)].⁴⁸ The excited-state lifetime obtained from the disappearance of these ν (CO) frequencies in solution decreases exponentially with the temperature: $\tau(T) = 356$ ns (195 K), 273 ns (206 K), 183 ns (217 K), 200 ns (228 K), 113 ns (238 K), and 108 ns (248 K). By fitting these temperature-dependent excited-state lifetimes to the Arrhenius equation ($1/\tau = Ae^{-E_a/RT}$), an estimated value of 800 cm⁻¹ (9.7 kJ mol⁻¹) is obtained for the activation energy.

(48) Clark, I. P.; George, M. W.; Johnson, F. P. A.; Turner, J. J. *Chem. Commun.* **1996**, 1587.

**Figure 7.** Time profiles of the intensities of the IR bands (CO-stretching region) belonging to the excited state (2029 cm⁻¹) and ground state (1987 cm⁻¹) of [Re(CH₃)(CO)₃(dmb)] and to the radical product [Re(Sv)(CO)₃(dmb)]* (2012 cm⁻¹) at 195 and 238 K.

Notably, this activation energy is, within the experimental error, close to that determined from the temperature-dependence of the emission lifetime (620 cm⁻¹).

Apart from the excited-state bands, two extra ν (CO) bands at 2012 and 1899 cm⁻¹ are observed in the spectra measured in the temperature range of 193–248 K. These bands remain unaltered for at least 10 μ s. They are attributed to the [Re(Sv)CO₃(dmb)]* radical since their frequencies correspond to those of the radicals produced by the reduction of [Re(X)(CO)₃(bpy)] (X = halide).⁴⁹ Figure 7 shows the decay curves at 195 K (top) and 238 K (bottom) of the 2029 cm⁻¹ excited-state band, of the 2012 cm⁻¹ band of the radical, and of the 1989 cm⁻¹ band of the parent compound. These curves reveal that the decay of the excited state and the recovery of the ground state occur with the same rate at both temperatures. Importantly, the decay of the excited state is not accompanied by a concomitant increase of the radical concentration. Hence, the radicals are not formed out of this particular excited state, which, according to its CO-stretching frequencies, has a predominant ³MLCT character. Instead, the kinetic curve obtained at 2012 cm⁻¹ shows that the radical formation is fully completed within the instrument rise time, ca. 50 ns. The intensity of the asymptotic flat part of the 2012 cm⁻¹ curve shows that the quantum yield of radical formation is rather low at 195 K and almost two times higher at 238 K. This is also evident from the observation that recovery of the ground state as seen from the 1989 cm⁻¹ curve is less complete at 238 K. This observation is fully consistent with the observed increase of the quantum yield with the temperature (Table 1), and it further supports the assignment of the 2012 cm⁻¹ band to the radical product.

Continuous irradiation ($\lambda_{exc} = 457.9$ nm) at room temperature of a solution of [Re(CH₃)(CO)₃(dmb)] in EtCN/PrCN (4:5 v/v) gives rise to the formation of the same radical species (ν (CO), 2011 and 1899 cm⁻¹) as that observed in the TRIR experiments.

(49) van Outersterp, J. W. M.; Hartl, F.; Stufkens, D. J. *Organometallics* **1995**, *14*, 3303.

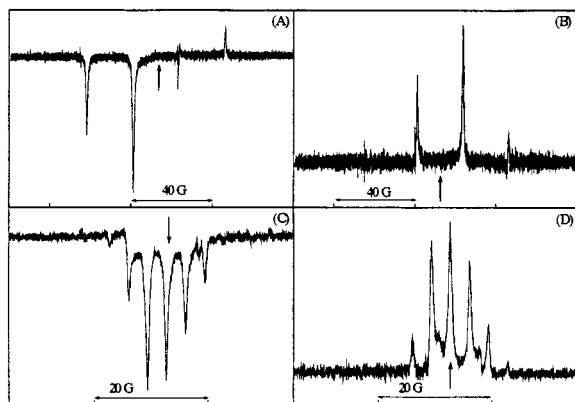


Figure 8. FT-EPR spectra of the CH_3 and CD_3 radicals produced by laser pulse excitation of $[\text{Re}(\text{R})(\text{CO})_3(\text{dmb})]$ in toluene. (A) $\text{R} = \text{CH}_3$, $\tau_d = 50$ ns. (B) $\text{R} = \text{CH}_3$, $\tau_d = 1 \mu\text{s}$. (C) $\text{R} = \text{CD}_3$, $\tau_d = 50$ ns. (D) $\text{R} = \text{CD}_3$, $\tau_d = 1 \mu\text{s}$. (The field increases from the left to the right.)

Apart from this radical species, two other $\nu(\text{CO})$ bands are observed at 2037 and 1933 cm^{-1} , which are assigned to the cation $[\text{Re}(\text{Sv})(\text{CO})_3(\text{dmb})]^+$.^{33,49}

Time-Resolved FT-EPR Spectra. To identify the radicals and to establish the spin character of the reactive excited state from which they are formed, a time-resolved FT-EPR spectroscopic study was undertaken. Representative spectra recorded after laser pulse excitation of the two $[\text{Re}(\text{R})(\text{CO})_3(\text{dmb})]$ ($\text{R} = \text{CH}_3$ or CD_3) complexes in toluene are shown in Figure 8. The spectra shown were measured for delay times between the laser and the microwave pulses of 50 ns and 1 μs , and are assigned to the CH_3 and CD_3 radicals. The hyperfine pattern of these spectra could be simulated with the following hyperfine splittings constant (hfsc) values: 22.7 (22.9) G ($\text{R} = \text{CH}_3$) and 3.3 (3.5) G ($\text{R} = \text{CD}_3$) in toluene (2-propanol), at a g -value of 2.002. The resulting hfsc's agree well with literature values for the CH_3 and CD_3 radicals ($a_{\text{H}} = 23.04$ G and $a_{\text{D}} = 3.576$ G in liquid methane).⁵⁰ The $a_{\text{H}}/a_{\text{D}}$ ratio of 6.9 (toluene) and 6.5 (2-propanol) are in good agreement with the theoretical value (6.5).

No EPR signals were observed from the $[\text{Re}(\text{CO})_3(\text{dmb})]^*$ radical complex, apparently because of a too-short T_2 , which causes the signal to decay within the spectrometer deadtime (ca. 100 ns). It was, however, possible to detect this radical with conventional EPR when a solution of $[\text{Re}(\text{R})(\text{CO})_3(\text{dmb})]$ ($\text{R} = \text{Et}$, Bz , or ^iPr) in glassy 2-MeTHF or 2-propanol at 133 K or in toluene at room temperature was irradiated within the EPR spectrometer. The $[\text{Re}(\text{Sv})(\text{CO})_3(\text{dmb})]^*$ radical manifests itself by broad (~ 30 G) peaks with g -values (2.005–2.008) slightly higher than those of the alkyl radicals (2.002).^{28,33,51} In agreement with the time-resolved absorption spectra of the $[\text{Re}(\text{R})(\text{CO})_3(\text{dmb})]$ complexes, which have shown that the photo-reaction completed within the 7 ns laser pulse, the rise time of the FT-EPR signals of the CH_3 and CD_3 radicals was instrument limited (40 ns). This result is also in accordance with our previous observations on other Re- and Ru-alkyl complexes.²⁸

The FT-EPR spectra show pronounced CIDEP effects (see Figure 8) at short delay times ($\tau_d = 50$ ns). In the case of the CH_3 radical, CIDEP gives rise to emission and absorption signals, while a totally emissive spectrum is observed for the CD_3 radical. The change in solvent from toluene to 2-propanol does not affect the CIDEP pattern. Concrete evidence that the signal intensities are determined primarily by CIDEP effects is

evident from the observation that the time evolution of the spectra during the first microsecond is controlled by spin–lattice relaxation, and that the spectra recorded at longer delay times ($\tau_d = 1 \mu\text{s}$) corresponds to a Boltzmann equilibrium, i.e., give rise to total absorption. The spin–lattice relaxation times are found to be: 89 ± 20 (101 \pm 40) ns (CH_3) and 103 \pm 20 (133 \pm 20) ns (CD_3) in toluene (2-propanol), respectively.

The spectra of the CH_3 radical exhibit a pronounced low-field-emission/high-field-absorption pattern with an overall net emission polarization (e^*/a pattern) both in toluene and 2-propanol. The e/a polarization is attributed to ST_0 radical pair mechanism (RPM) CIDEP generated in a triplet-state precursor radical pair.^{40,52,53} As noted above, the g -values of the CH_3^* and $[\text{Re}(\text{Sv})(\text{CO})_3(\text{dmb})]^*$ radicals that form the (weakly coupled) radical pair $^3[\text{CH}_3^* \dots [\text{Re}(\text{Sv})(\text{CO})_3(\text{dmb})]^*]$ are close in magnitude. Therefore, the RPM is predicted to give rise to an e/a pattern with the inversion center near the middle of the CH_3 radical spectrum.^{52,53} The deviation from this pattern (i.e. the net e polarization contribution) is attributed to triplet mechanism (TM) CIDEP.^{40,52,53} From the observation of these two CIDEP effects it can be concluded that a triplet excited state of $[\text{Re}(\text{CH}_3)(\text{CO})_3(\text{dmb})]$ must be the precursor of the free radical products. Because of its relatively small hyperfine splitting constant and the small difference in g -values of the two radicals, the RPM (e/a) contribution to the spectrum of CD_3 is small compared to the TM contribution. As a consequence the spectrum is completely in emission at short delay times (see Figure 8C).

Discussion

All complexes $[\text{Re}(\text{R})(\text{CO})_3(\text{dmb})]$ undergo the same photoreaction, viz. homolysis of the Re–R bond with the formation of the radicals $[\text{Re}(\text{CO})_3(\text{dmb})]^*$ and R^* . The complexes only differ in the efficiency of the reaction. Those in which $\text{R} = \text{Et}$, ^iPr , or Bz photodecompose with a quantum yield close to 1, the corresponding CH_3 complex has a quantum yield of only 0.4. In both cases the radicals are already formed within less than 10 ns and the time-resolved UV–vis and IR spectra do not give any spectral evidence for the reactive state from which the radicals are produced.

The quantum yield of 0.4 found for $[\text{Re}(\text{CH}_3)(\text{CO})_3(\text{dmb})]$ implies that 60% of the initially excited molecules decay to the ground state. The time-resolved UV–vis and IR spectra reveal that this unproductive decay occurs via a rather short-lived ($\tau = 40$ ns in toluene) excited state having a predominant $^3\text{MLCT}$ character. This MLCT character is evident from the observation that the replacement of the CH_3 group by CD_3 has no influence on the excited-state lifetime and mainly from the TRIR spectra, which show large shifts of the $\nu(\text{CO})$ vibrations to higher frequencies. At the same time, the emission spectra indicate a significant admixture of a $\sigma\pi^*$ character into the emissive state, in which σ represents the $\sigma(\text{Re}-\text{CH}_3)$ orbital. This is evident from the fact that the value of k_0 , derived from the temperature dependence of the emission lifetime, is only $6.5 \times 10^5 \text{ s}^{-1}$ ($E_{\text{em}} = 13\,800 \text{ cm}^{-1}$), whereas $k_0 = 5.4 \times 10^6 \text{ s}^{-1}$ for the typical $^3\text{MLCT}$ emission of $[\text{Re}(\text{Cl})(\text{CO})_3(\text{bpy})]$ ($E_{\text{em}} = 16\,180 \text{ cm}^{-1}$). These data show that the CH_3 and Cl complexes have a different character of their emissive excited state, since the rates of the nonradiative decay do not follow the energy gap law.^{5,44,54} The same is true for the emission from the low-temperature glasses,

(52) Trifunac, A. D.; Lawler, R. G.; Bartels, D. M.; Thurnauer, M. C. *Prog. React. Kinet.* **1986**, *14*, 43.

(53) McLauchlan, K. A. *Modern Pulsed and Continuous-Wave Electron Spin Resonance*; Kevan, L., Bowman, M. K., Eds.; Wiley: New York, 1990.

(54) Caspar, J. V.; Meyer, T. J. *J. Phys. Chem.* **1983**, *87*, 952.

(50) Fessenden, R. W.; Schuler, R. H. *J. Chem. Phys.* **1963**, *39*, 2147.

(51) Klein, A.; Vogler, C.; Kaim, W. *Organometallics* **1996**, *15*, 236.

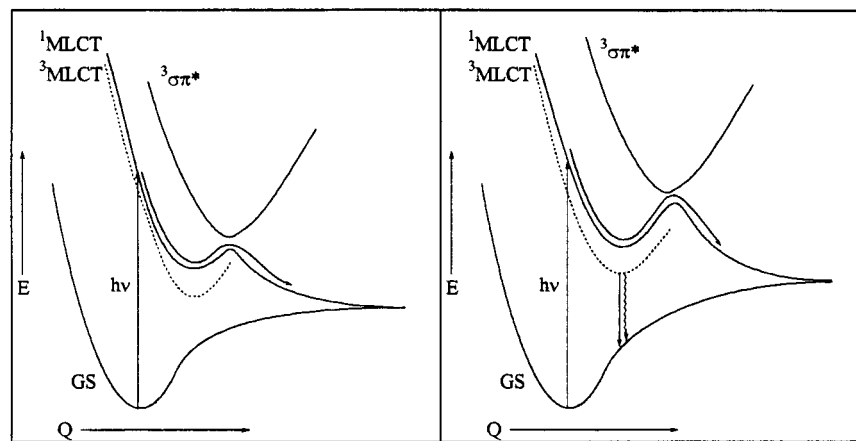


Figure 9. Schematic representation of the potential energy curves of the ground state, $^1\text{MLCT}$, $^3\text{MLCT}$, and $^3\sigma\pi^*$ states of $[\text{Re}(\text{R})(\text{CO})_3(\text{dmb})]$ with $\text{R} = \text{Et}$, Bz , and ^iPr (left) and $\text{R} = \text{CH}_3$ and CD_3 (right). Excitation into the $^1\text{MLCT}$ state is followed by crossing the barrier to the reactive $^3\sigma\pi^*$ state, from which the radicals are formed (see arrow). For $\text{R} = \text{Et}$, Bz , and ^iPr , this barrier is very low and radical formation is virtually the only photoprocess at room temperature. For $\text{R} = \text{Me}$, this barrier is much higher and only ca. 40% of the excited complex molecules photodecompose into radicals (arrow), while ca. 60% decay to the nonreactive $^3\text{MLCT}$ state and from there unproductively to the ground state.

since the nonradiative decay rate constant of $[\text{Re}(\text{CH}_3)(\text{CO})_3(\text{dmb})]$ is smaller than that of $[\text{Re}(\text{Cl})(\text{CO})_3(\text{bpy})]$ despite the much lower emission energy of the methyl complex (see Table 3). As the emissive excited state of the Cl complex has a $^3\text{MLCT}$ character, we tentatively conclude that the corresponding state of the CH_3 complex may have a mixed $^3\text{MLCT}/\sigma\pi^*$ character although the TRIR spectra point to a more or less “pure” $^3\text{MLCT}$ state. The longer than expected lifetime may be caused by weaker electronic coupling between the excited and ground states due to the $\sigma\pi^*$ admixture. Recent CASSCF/MR-CCI calculations on the ground and excited states of the model complex $\text{Re}(\text{H})(\text{CO})_3(\text{H-DAB})$ (H-DAB = 1,4-diazabutadiene) also point to a significant mixing between MLCT and $\sigma\pi^*$ states.⁵⁵

The long-lived transient that remains in the time-resolved spectra of $[\text{Re}(\text{CH}_3)(\text{CO})_3(\text{dmb})]$ after the decay of the $^3\text{MLCT}$ state belongs to the $[\text{Re}(\text{Sv})(\text{CO})_3(\text{dmb})]^*$ radical. It is not accidental that the visible absorption bands of this radical and the $^3\text{MLCT}$ state nearly coincide. Both species contain the dmb radical anion which has electronic transitions in this wavelength region.⁴³ The time-resolved spectra of $[\text{Re}(\text{CH}_3)(\text{CO})_3(\text{dmb})]$ measured from the fluid solution in both the UV-vis and IR regions show that the $^3\text{MLCT}$ state and the radical photoproduct are formed simultaneously within the duration of the excitation pulse, ca. 7 ns. However, because of the near coincidence of their visible transient absorption bands, it could not be excluded that part of the radicals was produced by the reaction from the $^3\text{MLCT}$ state. This question was solved by the TRIR spectra of $[\text{Re}(\text{CH}_3)(\text{CO})_3(\text{dmb})]$ measured in EtCN/PrCN (4:5 v/v) at 195 and 238 K. According to these spectra, the decay of the $^3\text{MLCT}$ state is not accompanied by any increase of the radical concentration. Instead, the $^3\text{MLCT}$ state was found to decay selectively to the ground state. Hence, the optical excitation into the $^1\text{MLCT}$ state is followed by two independent deactivation pathways, viz. a relaxation to a long-lived, emissive, $^3\text{MLCT}/\sigma\pi^*$ state and a crossing on a dissociative $^3\sigma\pi^*$ potential energy surface. The triplet character of this reactive $^3\sigma\pi^*$ state is evident from the time-resolved FT-EPR spectra of methyl radicals derived from $[\text{Re}(\text{CH}_3)(\text{CO})_3(\text{dmb})]$. These spectra show an emission/absorption ST_0 RPM/TM polarization pattern, implying that radical pair formation takes place via a triplet excited state.

On the basis of these observations and the results from the time-resolved spectra and quantum yield data, we can now construct a qualitative diagram of the potential energy curves of the ground state, the $^1,^3\text{MLCT}$ states and the dissociative $^3\sigma\pi^*$ state for the two different types of complexes, viz. $[\text{Re}(\text{R})(\text{CO})_3(\text{dmb})]$ ($\text{R} = \text{Et}$, ^iPr , Bz) on one hand, and $[\text{Re}(\text{CH}_3)(\text{CO})_3(\text{dmb})]$ on the other. These diagrams are depicted in Figure 9.

The diagram on the left represents the situation encountered for the ethyl, isopropyl and benzyl complexes, where MLCT excitation is followed by a nearly complete decomposition into radicals ($\Phi = 1$ at room temperature on 488.0 nm excitation, see Table 1). There is only a very small, wavelength dependent, barrier that most probably occurs between the $^1\text{MLCT}$ and $^3\sigma\pi^*$ states ($E_a = 215\text{--}330\text{ cm}^{-1}$). The situation is different for the corresponding methyl-complex (Figure 9, right). The $^1\text{MLCT}$ state has still about the same energy as in other alkyl complexes since the MLCT band hardly shifts on replacing the R group. On the other hand, the $^3\sigma\pi^*$ state is raised in energy for the methyl complex since the $\sigma(\text{Re}-\text{CH}_3)$ orbital has a higher ionization potential than the other $\sigma(\text{Re}-\text{R})$ orbitals.^{25,26} As a result, there is a larger barrier ($E_a = 1560\text{ cm}^{-1}$) between the $^1\text{MLCT}$ and $^3\sigma\pi^*$ states. After the excitation to the $^1\text{MLCT}$ state, the crossing of this barrier has to compete with the decay to the unreactive $^3\text{MLCT}$ state. As the intersystem crossing to the $^3\text{MLCT}$ state is expected to be very fast for this heavy-metal complex, surface crossing from the $^1\text{MLCT}$ state to the $^3\sigma\pi^*$ state will only compete with the decay to the $^3\text{MLCT}$ state, if that $^1\text{MLCT}$ state has an appreciable $\sigma\pi^*$ character. Indeed, recent CASSCF/MR-CCI calculations on the ground and excited charge transfer states of the model complex $\text{Re}(\text{H})(\text{CO})_3(\text{H-DAB})$ indicate that the Franck-Condon $^1\text{MLCT}$ state has a high contribution from the $\sigma(\text{Re}-\text{H}) \rightarrow \pi^*(\text{H-DAB})$ excitation.⁵⁵

In view of the disappearance quantum yield and the time-resolved spectra, there is a ca. 40% probability for crossing the barrier and radical formation and ca. 60% for decay to the $^3\text{MLCT}$ state and from there to the ground state. The transition from the $^3\text{MLCT}$ state to the $^3\sigma\pi^*$ does not occur, most probably because the barrier between these states is too large. Comparing the behavior of this dmb complex with that of the corresponding $[\text{Re}(\text{CH}_3)(\text{CO})_3(^i\text{Pr-DAB})]$ compound, the most striking difference is the much lower quantum yield for the latter complex ($\Phi = 3 \times 10^{-2}$ at 457.9 nm excitation) although the barrier between the $^1\text{MLCT}$ and $^3\sigma\pi^*$ states is only 627 cm^{-1} at this

(55) Guillaumont, D.; Wilms, M. P.; Daniel, C.; Stufkens, D. J. *Inorg. Chem.* In press.

wavelength. Apparently, the unproductive relaxation of the initially populated vibronic levels of the $^1\text{MLCT}$ state is much faster for the ^iPr -DAB complex than in the case of the dmb compound, diminishing strongly the efficiency of the barrier crossing.

The emission lifetime of $[\text{Re}(\text{CH}_3)(\text{CO})_3(\text{dmb})]$ was studied as a function of temperature in the glass-to-fluid transition region and at higher temperatures, at which there was still no photodecomposition into radicals. From this temperature dependence, an activation energy of 620 cm^{-1} is derived. This E_a does not represent the barrier to a reactive state, but to another nonreactive excited state, most probably also of an MLCT character, which decays more rapidly and nonradiatively to the ground state. A similar temperature-dependent nonradiative decay has been observed for the MLCT states of other diimine complexes of Re^{I} , Os^{II} , or Ru^{I} .^{5,56,57} Notably, the large difference between the values of the activation energies obtained from the temperature dependencies of the quantum yield and the emission lifetime presents additional evidence for the fact that the emissive state is not involved in the photochemical reaction.

Although the excited-state UV-vis absorption of $[\text{Re}(\text{CH}_3)(\text{CO})_3(\text{dmb})]$ is very similar in a glass and a fluid solution, the corresponding transient IR spectra are very different. Thus, the $^3\text{MLCT}$ state has $\nu(\text{CO})$ bands in the EtCN/PrCN (4:5 v/v) solution at 195 K at 2029, 1950, and ca. 1925 cm^{-1} , which shift to lower frequency, viz. 2014, 1933, and 1903 cm^{-1} , on going to the glass of this mixture at 80 K. A similar effect has been observed for the complex $[\text{Re}(\text{Cl})(\text{CO})_3(\text{bpy})]$ in the same solvent mixture.⁴⁸ Apparently, the relaxed excited state has a smaller charge separation in the glass than in fluid solution, whereby the $\nu(\text{CO})$ frequencies are less shifted with respect to

those of the ground state. This decrease of charge separation on going to the glass is probably due to the fact that, in this rigid medium, a stabilizing change of solvation is no longer possible.

Conclusions

From all metal-metal and metal-alkyl bound carbonyl- α -diimine compounds studied so far, the $[\text{Re}(\text{R})(\text{CO})_3(\text{dmb})]$ complexes give the most detailed information on the excited state processes leading to the formation of radicals. In the case of $\text{R} = \text{Et}$, ^iPr , and Bz , there is a direct propagation from the optically excited $^1\text{MLCT}$ state onto the dissociative $^3\sigma\pi^*$ potential energy surface, and the radicals are formed from thereon with nearly unit efficiency. The behavior of the $[\text{Re}(\text{CH}_3)(\text{CO})_3(\text{dmb})]$ complex is rather unique. The $^1\text{MLCT}$ Franck-Condon excitation is followed by two parallel deactivation pathways. One of them involves a thermally activated transition onto the $^3\sigma\pi^*$ potential energy surface and, ultimately, leads to the formation of the radical photoproducts by the $\text{Re}-\text{CH}_3$ bond homolysis. In the second, unproductive, deactivation pathway, a long-lived excited state of a mixed $^3\text{MLCT}/\sigma\pi^*$ character is populated, which then decays to the ground state both radiatively and nonradiatively. This excited state is not involved in the photochemistry. The branching ratio between the photochemical and unproductive deactivation pathways is ca. 0.4:0.6, at room temperature, giving rise to a photochemical quantum yield of ca. 0.4.

Acknowledgment. Financial support from The Netherlands Foundation for Chemical Research (SON), The Netherlands Organization for the Advancement of Pure Research (NWO), and the COST D4 Action is gratefully appreciated. H.v.W. acknowledges financial support for this work by the Division of Chemical Sciences, Office of Basic Energy Sciences of the US Department of Energy (DE-FG02-84ER-13242).

(56) Lumpkin, R. S.; Kober, E. M.; Worl, L. A.; Murtaza, Z.; Meyer, T. *J. J. Phys. Chem.* **1990**, *94*, 239.

(57) Nieuwenhuis, H. A.; Stufkens, D. J.; Vlček, A., Jr. *Inorg. Chem.* **1995**, *34*, 3879.